山口大学教育学部研究論叢　第74巻　153頁～162頁　2025年3月

Effects of Nodal Receptor Inhibition during Embryonic Stages of Development in Two Temnopleurid Sea Urchins

SAKAGUCHI Chikara*, KASAHARA Mami*, YAMANAKA Akira**, KITAZAWA Chisato*, ***

（Received September 27, 2024）

During the development of many animals, Nodal signaling is crucial for the specification of the embryonic axis. In sea urchin development, Nodal signaling also regulates dorso-ventral and left-right axis formation. Recently, we reported that temnopleurid sea urchins form an adult rudiment in a manner that differs from that in many other species, in which the mechanism of establishment of the embryonic axes is dependent on Nodal, and is highly conserved. However, the effects of Nodal inhibition during the embryonic stages on the subsequent larval stages are known. In the present study, we analyzed the effects of Nodal receptor inhibition on larval development of two temnopleurids, *Temnopleurus hardwickii* and *T. reevesii*. Larvae derived from Nodal receptor-inhibited embryos exhibited an abnormal skeletal pattern with a narrower space between the body rods at the dorsal apex. Their digestive organs were straight rather than curved but retained some functionality. At metamorphosis, the larvae retained many pigment cells and formed an adult rudiment with many more tube feet than controls. These observations indicate that the effects of Nodal inhibition during the embryonic stages, on the body axes and cell movement, continue into the larval stages.

KEY WORDS: Temnopleurid sea urchins, Nodal receptor inhibition, Larval development.

BACKGROUND

Nodal, a member of the transforming growth factor-ß (TGF-ß) superfamily, plays a key role in the specification of the embryonic axis of many animals. Furthermore, in sea urchin development, it is a conserved factor in establishing the dorso-ventral (DV) and left-right (LR) axes (Molina et al., 2013; Duboc et al., 2004, 2005; Bessodes et al., 2012). Nodal expression is caused by maternal Oct1/2 and zygotic Vg1/Univin expression in the presumptive oral ectoderm around the 60–128-cell stages (Range and Lepage, 2011). At the mid-gastrula stage, asymmetric *nodal* expression is induced at the right archenteron tip by Univin and Nodal at the ectoderm, and by BMP at the left archenteron with FGF and ERK, with final asymmetric expression of *nodal* at

＊　山口大学教育学部，〒753-8513，山口市吉田 1677-1，chisak@yamaguchi-u.ac.jp，　***山口大学大学院東アジア研究科

**　山口大学理学部生物学科，山口大学大学院創成科学研究科

the tip of the right archenteron inducing oral ectodermal expression to the right side (Bessodes et al., 2012). When Nodal signaling was inhibited in *Paracentrotus lividus* by injection of morpholino and treatment with the Nodal/Activin receptor inhibitor SB431542 (Alk4/5/7 receptor inhibitor) (Inman et al., 2002), specimens became radialized without a larval mouth and displayed altered LR asymmetry (Duboc et al., 2005).

Nodal also regulates the FGFA/FGFR pathway, which is needed for patterning of primary mesenchyme cells (PMCs) and gastrulation (Röttinger et al., 2008), especially where late Alk4/5/7 signaling is required for anterior skeletal patterning during gastrulation (Piacentino et al., 2015). Duboc et al. (2010) also indicated that a balance between ventralising Nodal and dorsalising BMP2/4 controls patterning of three germ layers as an organising center. Nodal causes DV patterning of secondary mesenchyme cells (SMCs), i.e., blastocoelar cells ventrally and pigment cells dorsally. Using *Hemicentrotus pulcherrimus*, Ohguro et al. (2011) indicated that Nodal inhibition resulted in decreased numbers of blastocoelar cells, coelomic pouch cells and circum-esophageal muscle cells, and increased numbers of pigment cells and spicule tip cells. Therefore, during the process of specification of SMCs, when the lower tiers of descendants of veg2 receive Delta signals from the micromere descendants, they are first specified as precursor cells of pigment and blastocoelar cells. The oral group of these cells are exposed to the Nodal signal and then become blastocoelar cells, while the aboral group are specified as pigment cells. When the middle tier receives Nodal signaling, the coelomic pouch and muscle precursor cells are specified, while the precursor cells of the spicule tip cells may be specified without exposure to Nodal. Therefore, Nodal signaling plays a critical role in specification process of five types of SMCs (Duboc et al., 2004, 2010; Flowers et al., 2004; Ohguro et al., 2011).

The molecular bases of these developmental events are being investigated in some common sea urchin species. Recently, we have focused on temnopleurids because they acquire features from that differ from those of common species during development. For example, temnopleurid species form an adult rudiment derived from the cell mass (CM) of the left larval body at the early larval stage (Fukushi, 1959; Kitazawa et al., 2012, 2014), whereas other species commonly form the rudiment derived from the amniotic cavity at the late larval stage. It was reported that the position of the CM is also controlled by H^+/K^+-ATPase (Kitazawa et al., 2013) and Nodal signaling (Kasahara et al., 2018). Furthermore, we observed that Nodal inhibition until the early larval stage altered DV and LR patterning in four temnopleurids, including *Mespilia globulus*, *Temnopleurus toreumaticus*, *T. hardwickii*, and *T. reevesii* (Kasahara et al., 2018). These findings suggest that the development of temnopleurids is based on common molecular events, despite different adult rudiment formation. In considering the acceleration of adult rudiment formation induced by CM formation in these species, it is unknown whether there are other effects of Nodal inhibition on adult traits, or whether the effects of Nodal inhibition on the embryonic stages are retained during larval development.

Therefore, in this study we focused on the effects on larval development of Nodal inhibition during embryonic stages in *T. hardwickii* and *T. reevesii*.

MATERIALS AND METHODS

Culture and Nodal Inhibition

Adult temnopleurids, *T. hardwickii* and *T. reevesii*, were collected from the Setonai Inland Sea, Yamaguchi Prefecture, Japan. A small volume of 0.5 M KCl solution was injected into the body cavity to induce spawning. The eggs were washed in several

changes of filtered sea water, and then fertilized. The fertilized eggs were cultured in plastic dishes containing artificial sea water (ASW; TetraMarin® Salt Pro, Tetra, Melle, Germany) at 24℃. When the specimens had formed a larval mouth, approximately 50 specimens were transferred to 50-mL plastic tubes filled with ASW and a few drops of ASW containing *Chaetoceros gracilis* diatoms as the larval food, and a small air bubble to stir the culture water, according to Kitazawa et al. (2012), with some modification. The culture tubes were shaken horizontally 70 times/min in a plastic tray fixed to a double shaker (NR-3, TAITEC, Saitama, Japan) at 24℃. The culture water was replaced every 3 days with new ASW containing food.

Specimens were observed under microscopes (ECLIPSE E-200 and OPTIPHOT-2, Nikon Instruments, Tokyo, Japan) and a stereomicroscope (SZ61, Olympus Corporation, Tokyo, Japan), and photographed using digital cameras (DS-Fil, Nikon; STYLUS XZ-10, Olympus).

At each developmental stage, aliquots of specimens were incubated in 0.1% dimethyl sulfoxide (DMSO)-ASW containing 5–10 μM of SB431542 (Sigma-Aldrich; Merck KGaA. Darmstadt, Germany), a Nodal receptor inhibitor to inhibit TGF-ß superfamily type I activin receptor-like kinase (Alk) receptor Alk4/5/7 (Inman et al., 2002). After treatment, the specimens were rinsed twice with ASW and transferred to new plastic dishes for culturing until larval mouth opening.

A portion of the specimens was fixed with 4% formaldehyde-ASW for approximately 1 h, rinsed, and then transferred into 70% EtOH. The fixed specimens were rinsed with distilled water for a few minutes and then observed and photographed under the microscopes

Scanning Electron Microscopy of the Larval Skeleton

Aliquots of larvae were laid onto a nano-percolator (4KA0122-00, JEOL Corporation, Tokyo, Japan) and rinsed with distilled water to burst the cells. Drops of 40% KOH solution were added for several minutes to remove organic substances, and then the larval skeletal samples were rinsed with distilled water and dried. Finally, after coating with gold using an ion sputter device (E-1010, Hitachi High-Technologies, Tokyo, Japan), specimens were observed and photographed under a scanning electron microscope (Miniscope TM-1000S, Hitachi High-Technologies).

RESULTS

Previously, we analyzed the effects on embryonic development, and on the LR polarity of the CM, of Nodal receptor inhibition by SB431542 treatment in temnopleurids (Kasahara et al., 2018). In the present study, we focused on the effects on larval development of SB431542 treatment in *T. hardwickii* and *T. reevesii*. After the embryos were treated with ASW containing 5–10 μM of SB431542 each period, we observed abnormal morphological features in the larval skeleton, changes in the number of pigment cells, elongation of the digestive organ and changes in number of tube feet in the adult rudiment as shown in Kasahara et al. (2018) (Figs.1–3). As shown in the previous report, the effects were dose-dependent (data not shown). Control embryos were treated with 0.1% DMSO-ASW, showed normal morphology (Fig.3H, I).

Effects of SB431542 Treatment on the Larval Skeleton

Observation of the larval skeleton during 3–10 days after fertilization revealed at least three patterns, depending on the period of Nodal receptor inhibition: most of the larval skeleton or the fenestrated post-oral rods did not form (Fig. 1A–C); only a post-oral rod formed (Fig. 1D); or

the width between the post-oral arms at the tip was narrower (Fig. 1E) than in the controls (Fig. 1F). Also, the body rods at the posterior end obtained numerous long spines (Fig. 1G). Treatment with the higher dose of the inhibitor also caused development to be arrested at this stage. Treatments for 0–10 h (during fertilization to the blastula stage), 11–21 h (during the mesenchyme blastula to prism stages), and 12–21 h or 13–23 h after fertilization resulted in lower survival rates among the specimens without post-oral rods (Table 1). Treatments for 14–24 h (during the early-gastrula to prism stages) and 16–26 h after fertilization resulted in larvae with a post-oral rod either on both sides (16.7% and 66.6%, respectively) or on one side only (12.5% and 16.7%, respectively). Treatment for one hour during 14–19 h after fertilization resulted in a larger proportion that formed a post-oral rod on both sides, than long term treatments commenced during the period. In *T. reevesii*, long-term treatment at the early stage inhibited larval skeletogenesis, but treatment between the mesenchyme-blastula and prism stages allowed 11.8% of the larvae to form a post-oral rod on one side (Table 1). Treatments for one hour at 11–15 h after fertilization increased the proportion of larvae that formed a post-oral rod on both sides. In scanning electron microscope observations of the larval skeletons (Fig. 1H–K), specimens of *T. hardwickii* treated during 15–25 h after fertilization did not exhibit ventral-transverse or recurrent rods, but displayed two body rods. Additionally, the post-oral rod of these specimens was shorter (Fig. 1I) compared with controls (Fig. 1H) and the body rods grew numerous spines at the dorsal apex. In *T. reevesii* (Fig. 1J, K), specimens treated with SB431542-ASW between the early- and mid-gastrula stages did not exhibit elongated antero-lateral rods (Fig. 1K), but presented two body rods and ventral-transverse rods that were elongated in different directions. The body rods also grew numerous spines at the dorsal apex.

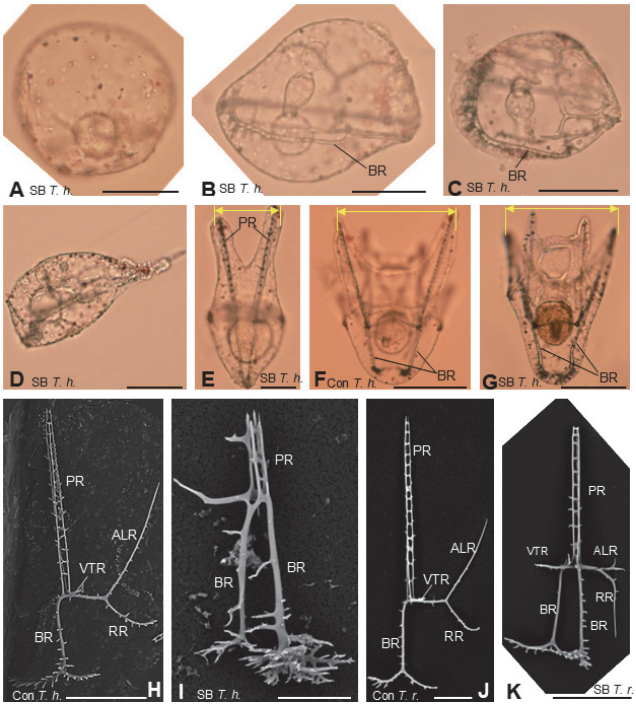

Fig. 1. Effects of Nodal receptor inhibition during embryonic stages on skeletogenesis in temnopleurids. Embryos and larvae of *Temnopleurus hardwickii* (*T. h.*) (A–I) and *T. reevesii* (*T. r.*)(J, K) are shown in light micrographs (A–G) and scanning electron micrographs (H–K). (A–C) Specimens derived from embryos treated 11–21 h after fertilization with SB431542-ASW were observed 4 days after fertilization (because of their abnormal morphology it was unclear whether they are viewed from the anal or abanal aspect). (D) A specimen with only one larval arm 4 days after fertilization, derived from an embryo treated with SB431542-ASW 14–24 h after fertilization, viewed from the lateral aspect. (E–G) Larvae observed 10 days after fertilization. A larva derived from an embryo treated with SB431542-ASW 14–18 h after fertilization (E: anal view) showing the narrow area formed between the post-oral arms (yellow double-sided arrow). In the non-treated control (F: anal view), a larva derived from an embryo treated with SB431542-ASW 15–20 h after fertilization (G: anal view) had numerous long spines at the dorsal apex of the body rods. (H–K)

Larval one-sided skeletons 2–3 days after fertilization, with controls (H, J) and specimens 3 days after fertilization derived from embryos treated with SB431542-ASW 15–25 h (I) or 14–24 h (K) after fertilization, in lateral view. Nodal inhibition caused abnormal elongation (or patterning) of the larval skeletons, especially in *T. h*. which lacks ventral-transverse and recurrent rods (I). *T. r*. exhibits short antero-lateral rods and the two body rods with many spines (I, K). ALR: antero-lateral rod; BR: body rod; PR: post-oral rod; RR: recurrent rod; VTR: ventral-transverse rod. SB: specimen derived from SB431542-ASW-treated embryo. Con: control specimen. Scale bars=100 µm.

Table 1. Effects of Nodal receptor inhibition on the formation of post-oral rods

Period for inhibition after fertilization (h)	*n**	Survival rate (%)	Formation of the post-oral rods (%)		
			Both sides	One side	Non
T. hardwickii					
Control**	300	99.7	99.7	0	0.3
0–10	50	0	-	-	-
11–21	50	12.0	0	0	100
12–21	50	28.0	2.0	2.0	96.0
13–23	50	10.0	0	0	100
14–24	50	48.0	16.7	12.5	80.8
16–26	50	12.0	66.6	16.7	16.7
14–15	50	10.0	40.0	40.0	20.0
17–18	50	12.0	66.7	33.3	0
18–19	100	32.0	71.9	25.0	3.1
T. reevesii					
Control**	54	98.1	100	0	0
0–10	100	21.0	0	0	100
11–21	100	34.0	0	11.8	88.2
11–12	150	74.7	20.6	8.0	71.4
12–13	100	85.0	91.8	2.3	5.9
14–15	150	30.0	53.3	15.6	31.1

*Specimens were observed 3–4 days after fertilization. The data are based on totals of 6 and 4 experiments for *T. hardwickii* and *T. reevesii*, respectively. **Control were specimens cultured in ASW.

Other Morphological Effects in Larval Development Caused by SB431542 Treatment

Nodal receptor inhibition during gastrulation generated an abnormal number of pigment cells and elongation of the digestive organ in *T. hardwickii*, as observed in *H. pulcherrimus* and some temnopleurid sea urchins (Ohguro et al., 2011; Kasahara et al., 2018; Suzuki and Yaguchi, 2018). Because it was unclear whether these features persisted until the later developmental stages, we continued to observe the specimens treated with SB431542-ASW (for *T. reevesii*, we had insufficient adults for this aspect of the study).

When the specimens treated with SB431542-ASW had formed a larval mouth, they survived by feeding. Some specimens treated with SB431542-ASW for a period after mid-gastrula stage developed straighter and more elongated digestive organs 2 days after fertilization, in comparison with controls (e.g., all specimens derived from embryos treated with SB431542-ASW for 10–20 h after fertilization formed straight and elongated of digestive organs, n = 11) (Figs. 2A, 3, Table 2). Many specimens developed a swollen intestine (Figs. 2A and 3E, G) (the ratio of length along the anterior-posterior axis for the width of an intestine was 1.1 ± 0.4 in specimens treated with SB431542-ASW during 0–10 h after fertilization, n = 8, 0.9 ± 0.1 for 10–20 h after fertilization, n = 3, 1.1 ± 0.2 for 20–30 h, n = 3, 2.1 ± 0.3 in specimens treated with DMSO-ASW during 10–20 h after fertilization, n = 6, respectively). At this stage, the controls exhibited curved digestive organs, and thus, the intestine was not observed wholly with in the same plane from the anal-abanal side (Figs 1F, 3H: views from the anal and abanal sides) (Fig. 3I: a view from the left lateral side).

Table 2. Effects of Nodal receptor inhibition during embryonic stages on endo-mesoderm development in *Temnopleurus hardwickii*

Period for inhibition after fertilization (h)	*n**	Mean number of mesenchyme cells (SE)	Elongation of digestive organs (%)		Coelomic pouches enlarged (%)
			Curved	Straight	
Control***	23	112.0 ± 6.3	100	0	0
0–10	20	160.3 ± 12.8	0	100	80.0
10–20	11	73.0 ± 28.8**	0	100	100
20–30	15	166.4 ± 17.7	100	0	0

*Specimens were fixed 2 days after fertilization for observation. **In these specimens, many mesenchyme cells were aggregated and could not be counted individually.
***DMSO treatment for 0–10 h after fertilization.

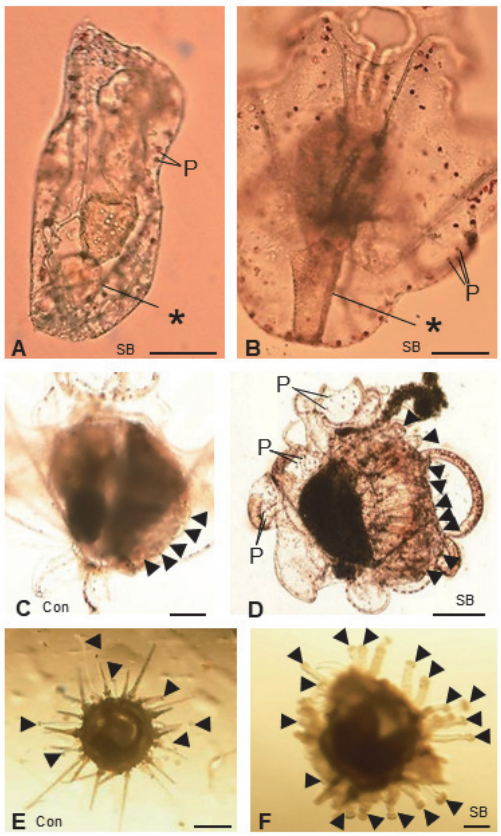

Fig. 2. Effects of Nodal receptor inhibition during embryonic stages on the larval development of *Temnopleurus hardwickii*. (A, B) Larvae 3 days (A) and 15 days (B) after fertilization, derived from embryos treated with SB431542-ASW 15–20 h after fertilization, viewed from the anal side. The digestive organs are formed linearly and the intestine is enlarged. Numerous pigment cells are present. (C, D) Larvae 27 days (C) and 25 days (D) after fertilization viewed from the anal side. The control larva (C) displays ca. 15 tube feet, and a larva derived from an embryo treated with SB431542-ASW for 5 min 18 h after fertilization (D) displays numerous (ca. 35) tube feet. (E, F) Juveniles viewed from the aboral side. A control 5 days after metamorphosis developed ca. 18 tube feet (E), whereas a metamorphosing specimen derived from an embryo treated with SB431542-ASW for 5 min 18 h after fertilization, acquired ca. 32 tube feet (F). SB: specimen derived from SB431542-ASW-treated embryo. Con: control specimen. Arrowheads: tube feet. Asterisks: intestine. P: pigment cells. Scale bars=100 μm.

After about 2 weeks culture, treated specimens still retained straight-elongated digestive organs (Fig. 2B). Some food was identified in the straight-elongated digestive organs and larval size increased, which implies that these organs acquired some digestive function. Treatment until 20 h after fertilization caused straight elongation of the digestive organs but the treatment after this stage did not cause this change. Basically, treated larvae exhibited large numbers of pigment cells than observed controls. The numbers of free mesenchyme cells 2 days after fertilization were higher in those treated with SB431542-ASW than in the DMSO controls, except for the treatment during 10–20 h (because the pigment cells were bleached after fixing with formaldehyde-ASW, we counted the total number of mesenchyme cells) (Table 2). In these specimens treated with SB431542-ASW, the mesenchyme cells gathered together into small masses and so the number of free mesenchyme cells apparently decreased (Fig. 3A, E). Larvae treated with SB431542-ASW retained numerous pigment cells until metamorphosis (Fig. 2D).

Thereafter, treated specimens formed adult rudiments at around 1 month, as did the controls. As shown by Kasahara et al. (2018), many specimens treated with SB431542-ASW around the time of coelomic pouch formation formed both CMs. However, some specimens derived from embryos treated with SB431542-ASW formed a CM only on the left side and developed more numerous tube feet compared with the controls (Fig. 2C, D). The number of tube feet was also higher in the metamorphosed juveniles (Fig. 2E, F), with 15 ± 5 tube feet in the rudiment of 8-armed larvae among controls (n = 6), and 35 ± 5 tube feet in larvae derived from SB431542-ASW-treated embryos (n = 9) 25 days after fertilization. To confirm the effects of SB431542-ASW treatment for the early embryonic stages, we reported the analysis of the effects on the coelomic pouches using fixed specimens (Fig. 3, Table 2). Treatment with SB431542-ASW until 20 h after fertilization caused cells to spread to form

the coelomic pouches (Fig. 3G, E). In some specimens, it was observed that the coelomic pouches did not separate to the left and right side (Fig. 3C). The treatment also caused enlargement of the coelomic pouches (Fig. 3D). However, treatment later than 20 h after fertilization caused larvae to form coelomic pouches on the left and right sides (Fig. 3F, G, Table 2).

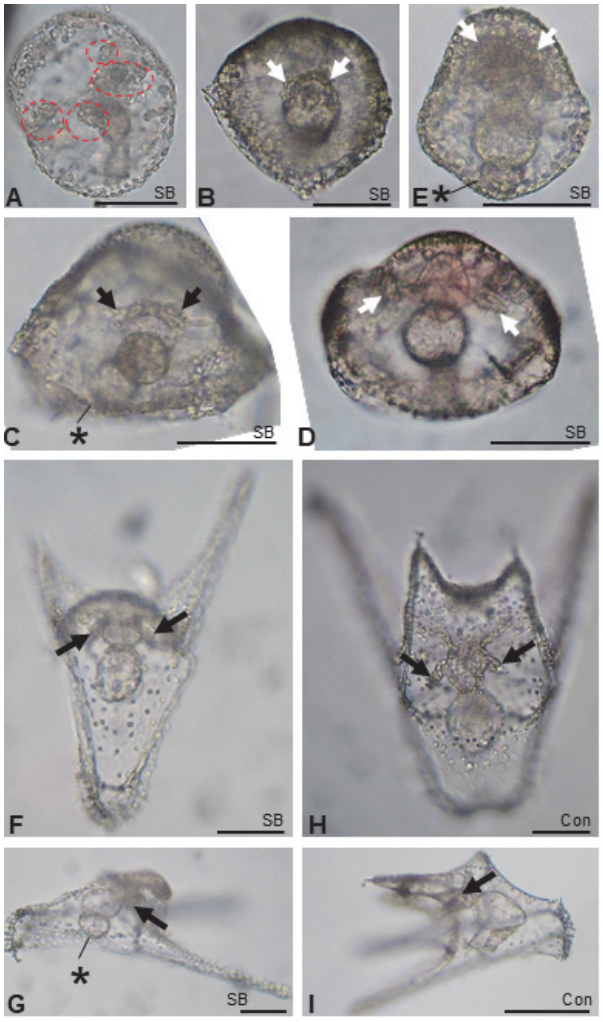

Fig. 3. Effects of Nodal receptor inhibition during embryonic stages on formation of coelomic pouches in *Temnopleurus hardwickii*. These specimens were fixed 2 days after fertilization. (A–D) Specimens derived from embryos treated with SB431542-ASW 0–20 h after fertilization. Half of the specimens generated many clumps of mesenchyme cells (red broken circles) (A) and other specimens formed coelomic pouches (B–D). The cells of the coelomic pouches spread over the tip of the archenteron (B) and formed large coelomic pouches (C, D). (E) A specimen derived from embryos treated with SB431542-ASW 10–20 h after fertilization. Numerous mesenchyme cells are present at the tip of the archenteron. (F, G) Specimens derived from embryos treated with SB431542-ASW 20–30 h after fertilization (F: abanal view, G: left lateral view). Large coelomic pouches are retained on both sides. (H, I) Control specimens derived from embryos treated with DMSO-ASW 0–10 h after fertilization (H: abanal view, I: left lateral view). Arrows: coelomic pouches or cells forming coelomic pouches. SB: specimen derived from SB431542-ASW-treated embryo. Con: control specimen. Asterisks: intestine. Scale bars=100 μm.

DISCUSSION

In this study, we analyzed the effects on larval development of SB431542 treatment during embryonic stages in *T. hardwickii* and *T. reevesii*. The treatment caused abnormal morphological features in the larval skeleton, straight elongation of the digestive organs, and increased numbers of pigment cells and tube feet in the adult rudiment. These observations suggest that Nodal inhibition effects cell movement in all of these phenomena.

With respect to the effects of SB431542 treatment on skeletogenesis, Alk4/5/7 may affect the regulation of patterning of PMCs, and, in turn, the formation of the larval skeleton. Kitazawa et al. (2016) showed that the precursor cells of PMCs, and ingression of PMCs, appear around 9 h and 9.5–10.5 h after fertilization, respectively, for *T. hardwickii* and 5.5–6 h and 7.5–8 h, respectively, for *T. reevesii*. Table 1 indicates that SB431542 treatment during at least these stages inhibited formation of the larval arms, implying that Nodal signaling regulates differentiation of PMCs. Also, the SB431542 treatment after PMC ingression caused inhibition of normal larval skeletogenesis. Inhibition of PMC patterning via Alk4/5/7 inhibition is implied by the reduced elongation of the post-oral rods and development of an abnormal number of spines at the tip of the body rods. This

indicates that, when the SB431542 treatment causes moderately severe effects on the body axes, the embryos are able to elongate the larval arms but are unable to develop normally; consequently, PMC patterning becomes abnormal. Because it is important for normal PMC differentiation for each PMC to communicate individually with the ectoderm (Armstrong et al., 1993; Hodor and Ettensohn, 1998), it is possible that Alk4/5/7 effects the ectoderm and its interaction with PMCs. Piacentino et al. (2015) indicated that late Alk4/5/7 signaling is required for anterior skeletal patterning during gastrulation, which is important for PMC patterning in other species. Specimens derived from embryos treated with SB431542-ASW from the mid-gastrula to prism stages did not form post-oral rods but formed adult reticulated skeletons, while the controls developed to the 6-armed stage (data not shown). This result suggests that larval skeletogenesis depends on Nodal signaling but that adult skeleton formation may be independent of Nodal. In addition, there were differences in the effects of Nodal inhibition between species, especially ventral-transverse rod and recurrent rod elongation (Fig. 1I, K). The reasons are unclear, but may relate to differences in the inhibitor effect on PMC patterning.

In the SB431542-treated specimens, elongation of the archenteron was straight with respect to differentiation of three sections of the digestive system, esophagus, stomach and intestine (Fig. 2A, B). In many sea urchin species, it is known that elongation of the archenteron requires towing of the gut rudiment by SMCs, which form filopodia (Gustafson and Kinnander, 1956). In embryos treated with SB431542-ASW during gastrulation, we considered that the treatment caused the patterning of the SMCs. Previous reports indicated that gastrula formation in *T. hardwickii* and *T. reevesii* occurred in a stepwise manner, with the first and secondary invaginations, and ingression of their SMCs starting around the end of the first invagination. Filopodia form during the secondary invagination (Kitazawa et al., 2016). Elongation of the archenteron stops in the middle of the embryonic body and then curves towards the oral side. Remarkably, it was considered that, in these species, elongation of the archenteron does not depend on towing by SMCs (Kitazawa et al., 2016). SB431542-ASW treatment after elongation of the archenteron to the middle of the embryonic body did not form the straight digestive organs (Table 2). Kitazawa et al. (2016) indicated that the elongation of archenteron of *T. hardwickii* and *T. reevesii* depends mostly on cell rearrangement, not by the positive effects of towing SMCs, based on measurements of each of the embryonic parts, the timing of ingression SMCs and formation of filopodia by SMCs. This implies that Alk4/5/7 directly effects the cell rearrangement of the archenteron. Suzuki and Yaguchi (2018) also indicated that the Alk4/5/7-phosphorylated-Smad2/3 pathway might mediate the cytoskeletal conformational change that bends the gut towards the mouth region in *H. pulcherrimus*. Straight elongation of the archenteron by inhibition of Alk4/5/7 has been observed in other sea urchin species (Duboc et al., 2004; Suzuki and Yaguchi, 2018) but survival of embryos with a straight-elongated archenteron has not been previously observed. In the present study, once the straight-elongated archenteron attached to the ectoderm, the archenteron differentiated into the digestive organs without curving. After differentiation of digestive organs, these larvae survived to metamorphosis (Fig. 2).

Furthermore, in the present study, SB431542 treatment caused an increase in the number of tube feet in *T. hardwickii* (Fig. 3). Although most of the effects of Nodal are common to other species, this is a new phenomenon associated with the role of

Nodal. When the embryos were treated with SB431542 during formation of the LR polarity, they formed two CMs and then formed an adult rudiment on both sides (Kasahara et al., 2018). Although the survival rate after SB431542 treatment in *T. hardwickii* was lower than in other species (Table 1) (Kasahara et al., 2018), it is possible that some larvae could survive with normal LR polarity to form an adult rudiment with many tube feet. Alternatively, these embryos may have disturbed differentiation of the left coelomic pouch, especially the hydrocoel, which increases the number of tube feet. Previously, Ohguro et al. (2011) indicated that Nodal inhibition caused a decrease in the number of coelomic pouch cells and increased the number of pigment cells before the commencement of gastrulation, but inhibition after this stage had no effect on *H. pulcherrimus*. Likewise, in the present study, it was observed that the number of pigment cells increased (Fig. 2B, D). Additionally, Fig. 3 and Table 2 show that the coelomic pouches became enlarged 2 days after fertilization. These results suggest that Nodal may inhibit the speed of coelomic pouch development and/or control branching of the hydrocoel into a maximum of five parts, to form the penta-radial symmetrically of the arms. It is also possible that Nodal controls the arrangement of coelomic pouch cells. In temnopleurids, differentiation of SMCs might be changed by heterochrony of adult rudiment formation to induce CM formation in the early larval stage.

ACKNOWLEDGEMENTS

We thank the Department of Fishery in Yamaguchi Prefecture and Yamaguchi Fisheries Cooperative Association. This work was financially supported in part by Yamaguchi University Foundation, JSPS KAKENHI Grant Numbers 19770195 to C. K. We thank Edanz for editing a draft of this manuscript.

REFERENCES

Armstrong, N., Hardin, J., and McClay, D. R. (1993) Cell-cell interactions regulate skeleton formation in the sea urchin embryo, Development, 119, 833-840.

Bessodes, N., Haillot, E., Duboc, V., Rottinger, E. and Lepage, T. (2012) Reciprocal signaling between the ectoderm and a mesendodermal left–right organizer directs left–right determination in the sea urchin embryo, PLoS Genet, 8(12), e1003121.

Duboc, V., Röttinger, E., Besnardeau, L. and Lepage, T. (2004) Nodal and BMP2/4 organizes the oral-aboral axis of the sea urchin embryos, Dev Cell, 6, 397-410.

Duboc, V., Röttinger, E., Lapraz, F., Besnardeau, L. and Lepage, T. (2005) Left–right asymmetry in the sea urchin embryo is regulated by nodal signaling on the right side, Dev Cell, 9, 147-158.

Duboc, V., Lapraz, F., Saudermont, A., Bessodes, N., Mekpoh, F., Haillot, E., Quirin, M. and Lepage, T. (2010) Nodal and BMP2/4 pattern the mesoderm and endoderm during development of the sea urchin embryo, Development, 137, 223-235.

Flowers, V. L., Courteau, G. R., Poustka, A. J., Weng, W. and Venuti, J. M. (2004) Nodal /Activin signaling establishes oral-aboral polarity in the early sea urchin embryo, Dev Dyn, 231, 727-740.

Fukushi, T. (1959) On the cell mass observed on the left side of the pluteus of the sea urchin, *Temnopleurus hardwickii*, Bull Mar Biol St Asamushi, 9(3), 133-135.

Gustafson, T. and Kinnander, H. (1956) Microaquaria for time-lapse cinematographic studies of morphogenesis in swimming larvae and observations on sea urchin gastrulation, Exp Cell Res, 11(1), 36-51.

Hoder, P. G. and Ettensohn, C. A. (1998) The dynamics and regulation of mesenchymal cell fusion in the sea urchin embryo, Dev Biol, 199(1), 111-124.

Inman, G. J., FNicolás, J., Callahan, J. F., Harling, J. D., Gaster, L. M., Reith, A. D., Laping, N. J. and Hill, C. S. (2002) SB-431542 is a potent and specific inhibitor of transforming growth factor-β superfamily type I activin receptor-like kinase (ALK) receptors ALK4, ALK5, and ALK7, Mol Phar, 62, 65-74.

Kitazawa, C., Fujii, T., Egusa, Y., Komatsu, M. and Yamanaka, A. (2016) Morphological diversity of blastula formation and gastrulation in temnopleurid sea urchins, Biol Open, 5, 1555-1566.

Kasahara, M., Kobayashi, C., Sakaguchi, C., Miyahara, C., Yamanaka, A. and Kitazawa, C. (2018) Effects of Nodal inhibition on development of temnopleurid sea urchins, Evo Dev, 20, 1-99.

Kitazawa, C., Kobayashi, C., Kasahara, M., Takuwa. Y. and Yamanaka, A. (2012) Morphogenesis of adult traits during the early development of *Mespilia globulus* Linnaeus, 1758, Zool Stud, 51(8), 1481-1489.

Kitazawa, C., Nakano, M., Kobayashi, C. and Yamanaka, A. (2013) Effects of ion flow on establishment of left-right polarity of the adult rudiment in larvae of *Temnopleurus toreumaticus*, Information, 17(1), 327-333.

Kitazawa, C., Skaguchi, C., Nishimura, H., Kobayashi, C., Baba, T. and Yamanaka, A. (2014) Development of the sea urchins *Temnopleurus toreumaticus* Leske, 1778 and *Temnopleurus reevesii* Gray, 1855 (Camarodonta: Temnopleuridae), Zool Stud, 53, 3.

Molina, M. D., de Croze, N., Haillot, E. and Lepage, T. (2013) Nodal: master and commander of the dorsal-ventral and left-right axes in the sea urchin embryo, Curr Opin Genet Dev, 23(4), 445-53.

Ohguro, Y., Tanaka, H. and Kominami, T. (2011) Involvement of Delta and Nodal signals in the specification process of five types of secondary mesenchyme cells in embryo of the sea urchin, *Hemicentrotus pulcherrimus*, Dev Growth Differ, 53, 110-123.

Piacentino, M. L., Ramachandran, J. and Bradham, C. A. (2015) Late Alk4/5/7 signaling is required for anterior skeletal patterning in sea urchin embryos, Development, 142, 943-952.

Range, R. and Lepage, T. (2011) Maternal Oct1/2 is required for Nodal and Vg1/Univin expression during dorsal-ventral axis specification in the sea urchin embryo, Dev Biol, 357, 440-449.

Röttinger, E., Saudemont, A., Duboc, V., Besnardeau, L., McClay, D. and Lepage, T. (2008) FGF signals guide migration of mesenchymal cells, control skeletal morphogenesis of the skeleton and regulate gastrulation during sea urchin development, Development, 135,353-365.

Suzuki, H. and Yaguchi, S. (2018) Transforming growth factor-ß signal regulates gut bending in the sea urchin embryo, Dev Growth Differ, 60, 216-225.